JOURNAL OF GUIDANCE, CONTROL, AND DYNAMICS
Vol. 18, No. 5, September–October 1995

# Flexible Vehicle Control Using Quantitative Feedback Theory

R. A. Hess* and D. K. Henderson†
*University of California, Davis, Davis, California 95616*

**The design of a longitudinal pitch-axis flight control system for a flexible aircraft with uncertainty in the vehicle model is presented. This uncertainty includes the characteristics of the vehicle elastic mode. Quantitative feedback theory is used in the control system design. A level 1 handling qualities requirement is included in the control systems design specifications. This requirement is generated through pilot–vehicle analysis using a structural model of the human pilot and handling qualities sensitivity functions. Although two aerodynamic controls were available (elevator and forward vane), it is shown that elevator control alone can be used to meet the command-following, disturbance rejection, and handling qualities requirements.**

## Nomenclature

$[d\Phi/dx]_{cp}$ = slope of body bending mode shape evaluated at pilot's station
$q$ = $d\theta/dt$, rad/s
$u$ = perturbation of $x$ body axis component of vehicle velocity, ft/s
$\alpha$ = angle of attack, rad
$\delta_c$ = canard angle (positive trailing edge down), deg
$\delta_e$ = elevator angle (positive trailing edge down), deg
$\eta$ = generalized modal coordinate for symmetric body bending mode
$\theta$ = pitch attitude of rigid body, rad

## I. Introduction

THE design of robust control systems is of continuing interest to the aircraft flight control community.[1,2] The interest is stimulated in part by the challenges associated with the control of high-speed vehicles in flight regimes where system dynamics can be highly uncertain and the assumptions of vehicle rigidity can no longer be employed.[3]

For flight modes in which the pilot is acting as a primary or back-up controller, design constraints associated with acceptable vehicle handling qualities must also be considered and are often the driver behind overall system performance requirements.[4]

To address these issues, an application of quantitative feedback theory (QFT) to the design of a longitudinal pitch-axis flight control system to a highly flexible vehicle with considerable uncertainty in the vehicle dynamic model is considered. This uncertainty includes the characteristics of the vehicle elastic mode. Vehicle handling qualities requirements as generated through pilot–vehicle analyses are included in the design specifications.

## II. Vehicle Model

The nominal vehicle model is an amalgam of the data found in Refs. 5 and 6 for the vehicle based upon the B-1 aircraft. The aerodynamic force and moment data were taken from Ref. 5, as was information on the mode shape of the symmetric body-bending mode. Aerodynamic structural data for the body-bending mode were, however, taken from Ref. 6. The data of Refs. 5 and 6 involved a vehicle model for a flight simulation study that addressed the effects of structural flexibility on the dynamic characteristics of a generic family of aircraft representative of advanced transports. Thus, the model presented here should be considered only as representative of a general class of aircraft and not as a model representative of the B-1 itself. This model was chosen solely because of the availability of the data.

Elastic degrees of freedom were limited to a single body-bending mode, as this was the only longitudinal elastic mode for which complete data were available. Two aerodynamic controls were available. One was a small forward vane, which for simplicity will simply be referred to as a canard herein, and the second was the elevator. The nominal flight condition was for Mach 0.6 at an altitude of 5000 ft. By assumption, only a single sensor is to be employed for the pitch-axis control system: a pitch-rate sensor mounted at the pilot's station. This station is near a node of the symmetric body-bending mode and represents less than an ideal location for a device sensing pitch rate. This was felt to provide something of a challenge to the design procedure to be discussed.

The vehicle equations of motion in state-space form are given in the Appendix, along with a definition of the variables involved. Although the canard was available, an elevator-alone design approach was followed. This also was felt to provide a challenge to the design procedure. Uncertainty in the vehicle dynamics was created artificially by considering four additional vehicle dynamic models each formed by perturbing elements of the $\boldsymbol{A}$, $\boldsymbol{B}$, and $\boldsymbol{C}$ matrices of the state equations. These additional state-space models are also included in the Appendix. As the Appendix indicates, actuator dynamics were also included in the study and were modeled as a first-order system with break frequency of 75 rad/s. This break frequency is considerably higher than the 10-rad/s value representative of the elevator actuator of the B-1.[7]

An example of the uncertainty created by this approach can be obtained by considering the frequency response diagrams for transfer functions relating pitch rate at the pilot's station ($q_{cp}$) to the elevator ($\delta_e$). This is shown in Fig. 1. Note the considerable variation in magnitude and phase, including that associated with the lightly damped structural mode. The uncertainty created in this fashion may be considered to arise from actual uncertainty as to the dynamic model of the aircraft at a specific flight condition and/or to variations in the vehicle dynamics as different flight conditions are encountered. Of course, were aerodynamic and structural data actually available for different flight conditions for this vehicle, the necessity of artificially creating uncertainty would be eliminated.

## III. Quantitative Feedback Theory Design

Although the QFT method has been described in the literature,[8] a brief description will be presented here for completeness. Consider the single-input, single-output (SISO) system shown in Fig. 2. QFT involves a two-degree-of-freedom design (elements $G$ and $F$ are obtained by the designer). The first degree of freedom is exercised in obtaining the loop transmission $L(j\omega) = G(j\omega)P(j\omega)$ so that the variation of the closed-loop frequency response over the frequency range of interest is within acceptable limits for all plants $P \in P_u$, where $P_u$ is the set of all possible plant variations created by uncertainty. The acceptable limits are obtained from time- or frequency-domain performance specifications that are interpreted

Received Aug. 23, 1993; revision received Dec. 10, 1994; accepted for publication Feb. 26, 1995. 

*Professor, Department of Mechanical and Aeronautical Engineering. Associate Fellow AIAA.

†Graduate Student, Department of Mechanical and Aeronautical Engineering.

in terms of bounds on the magnitude of the closed-loop frequency response.

The QFT technique can also be used for disturbance rejection, at either the plant input or the plant output. Including these disturbances transforms the SISO design into a multi-input, single-output (MISO) design, since two "inputs" are now in evidence, i.e., the command input and the disturbance input. Stability robustness is included in the QFT procedure by placing limits on $|L(j\omega)/[1 + L(j\omega)]|$ and $|1 + L(j\omega)|$. The latter requirement is synonymous with the specification of gain and phase margins.

The loop-shaping procedure is typically accomplished on a Nichols chart. This is done by selecting a $G(j\omega)$ so that at selected frequencies $\omega_j$ a "nominal" loop transmission $L_0(j\omega_j)$ lies above boundaries $B(j\omega_j)$. At each $\omega_j$, the $B(j\omega_j)$ are obtained using plant "templates" defining plant uncertainty and the following:

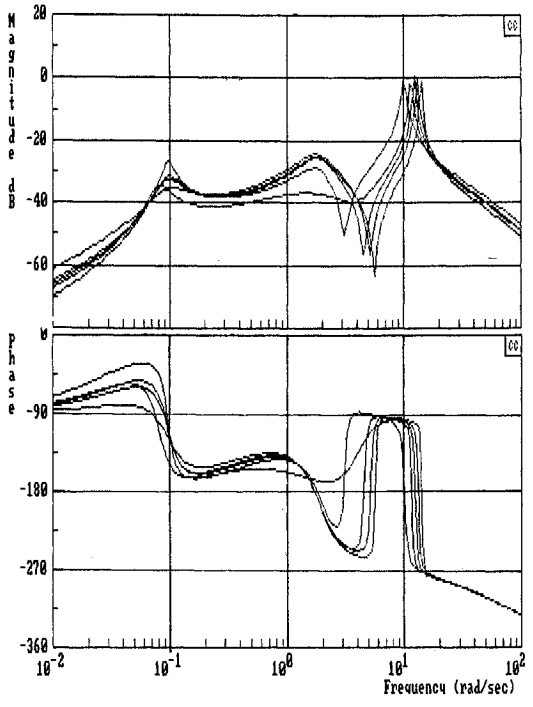


**Fig. 1** $(q_{cp}/\delta_e)(j\omega)$ **for five vehicle configurations of Appendix.**

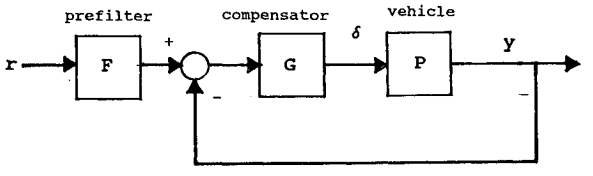


**Fig. 2 QFT SISO control system structure.**

maximum allowable variations in the command-following transfer function magnitudes, maximum magnitudes of output to injected disturbance transfer functions, and finally, stability margins, all of which constitute the quantitative design problem statement.

After $G(j\omega)$ has been obtained, the second degree of freedom is exercised in obtaining the prefilter $F(j\omega)$ so that the magnitudes of the closed-loop frequency response lie within the prescribed limits, i.e., the closed-loop transfer function $T \in T_a$ for all $P \in P_a$, where $T_a$ is the set of acceptable transfer functions, again obtained from the performance specifications. In this study, the QFT design was carried out using an efficient computer-aided design package.[9]

## IV. Predicting Handling Qualities

The structural model of the human pilot will be used to predict handling qualities levels.[4,10] The pilot–vehicle assessment technique will be used to initially suggest a desirable pitch-rate to pitch-rate command transfer function magnitude for the control system to produce and then will be used to assess the handling qualities of the five vehicle configurations that defined the uncertain vehicle dynamics.

### Handling Qualities Sensitivity Function

Figure 3 shows a control theoretic representation of the human operator referred to as the structural model.[10] The model has been divided into "central nervous system," "neuromuscular system," and "vestibular system," a division intended to emphasize the nature of the signal-processing activity involved. The displayed system error $e$ is presented to the pilot and multiplied by the gain $K_e$. If motion cues are available, output rate $m$ is assumed to be sensed by the vestibular system (provided it is an angular velocity or linear or angular acceleration). The output rate is multiplied by the gain $K_v$ and subtracted from the signal $u_e$. The resulting signal $u_1$ is passed through a central time delay $\tau_0$ intended to account for latencies in the visual process sensing $e$, motor nerve conduction times, etc.

The signal $u_c$ provides a command to a closed-loop system that consists of a model of the open-loop neuromuscular dynamics, $Yp_n$, of the particular limb driving the manipulator (control stick) and elements $Y_f$ and $Y_m$, which form two proprioceptive feedback loops in the structural model. It is this proprioceptive feedback that provides the basic equalization capabilities of the model and, by hypothesis, the human pilot. The form of $Y_m$ is determined by the order $k$ of the controlled element dynamics $Y_c$ in the region of the crossover frequency. Here crossover frequency refers to the frequency for which the magnitude of the loop transmission or open-loop transfer function is unity (0 dB).

By applying the structural model in a manner described and demonstrated in Ref. 10, the handling qualities level that would be assigned a particular vehicle and task can be predicted with reasonable success. The tool for accomplishing this prediction is the handling qualities sensitivity function (HQSF), defined as the

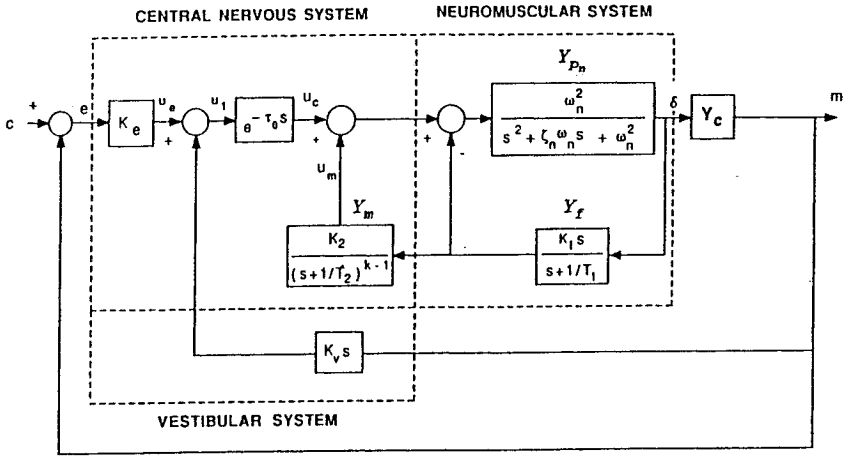


**Fig. 3 Structural model of human pilot.**

transfer function between the variable $u_m$ and $c$, i.e., $[(u_m/c)(s)]$ in Fig. 3. In particular, if $|(u_m/c)(j\omega)|$ remains below unity around the open-loop crossover frequency, the vehicle and task are predicted to have level 1 handling qualities. If $|(u_m/c)(j\omega)|$ exceeds unity around crossover, the vehicle and task are predicted to have level 2 ("deficiencies warrant improvement") handling qualities or worse. Details about determining structural model parameters and obtaining the HQSF are given elsewhere.[4,10]

## V. Control System Design

### Performance Requirements

*Command Following*

Figure 4 shows the bounds that will be assumed to define acceptable response characteristics for the pitch-rate command flight control system for the vehicle in question. These bounds were obtained as follows: The dashed line in the figure shows the magnitude of the transfer function

$$\frac{q_{cp}}{q_c}(s) = \frac{9}{(s+3)^2} \tag{1}$$

The dynamics of Eq. (1) were selected as those representing a rate-command system with moderate bandwidth (here approximately 3 rad/s). When these dynamics were used as an idealized pitch-rate command flight control system, it was found that level 1 handling qualities were predicted by the structural model using the methodology just described. In utilizing the HQSF, it was assumed that task performance required a crossover frequency of 0.75 rad/s. This value is not entirely arbitrary, representing, as it does, the frequency where phase lags in the transfer function of Eq. (1) begin to exceed 30 deg. Finally, with Eq. (1) representing a nominal system, the variations in magnitude as shown in Fig. 4 were allowed.

Obviously, there is considerable subjectivity here, especially in defining the allowable variations shown in Fig. 4. It was the authors' desire to use a preliminary pilot–vehicle analysis to provide some guidelines for performance specification. Bear in mind that the pilot models outlined in the preceding will be used to assess handling qualities for each of the five vehicle configurations defined in the Appendix after the control system design is complete.

*Disturbance Rejection*

It was also desired to place performance requirements on the turbulence response of the vehicle in question. Figure 5 shows a simplified block-diagram representation of the flight control system with disturbances. In modeling the aerodynamic effects of the turbulence, the vehicle was assumed to be moving through a one-dimensional upwash field, creating a gust perturbation in angle of attack $\alpha_g$. In this approach, the simplest treatment of the aircraft was undertaken; i.e., it was assumed that the entire aircraft experienced the upwash velocity existing at the aircraft center of gravity. By suitably modifying the vehicle equations of motion for flight through quiescent air in the Appendix, the aerodynamic effects of this one-dimensional upwash field could be easily represented[11] and the transfer functions $(q_{cp_g}/\alpha_g)(s)$ could be obtained for each configuration.

The disturbance rejection requirements for the QFT design are defined by requiring

$$\left|\frac{q_{cp}}{q_{cp_g}}(j\omega)_i\right| \le |T_d(j\omega)| \qquad i = 1, 2, \ldots, 5 \tag{2}$$

where $|T_d(j\omega)|$ represents some allowable maximum. The left-hand side of inequality (2) of course represents the magnitude of the sensitivity function $S_i(s)$ of the system of Fig. 5 with the $i$th vehicle configuration. Figure 6a shows the $|T_d(j\omega)|$ used here. This function was selected on the basis of estimates of the probable system complementary sensitivity functions and the relationship between the functions themselves, i.e., $T_i'(s) + S_i(s) = 1.0$, where $S_i(s)$ and $T_i'(s)$ refer to sensitivity and complementary sensitivity, respectively.[12] Here, the system complementary sensitivity is defined as $T'(s) = T(s)/F(s)$, where the $F(s)$ are the prefilter dynamics. Since these are unknown at this point, unity prefilter dynamics were assumed and the functions implied by Fig. 5 were used as initial estimates of the ranges of the complementary sensitivities of the closed-loop flight control systems.

Although Eq. (2) and Fig. 6a are used for the QFT design, it is $|(q_{cp}/\alpha_g)(j\omega)|$ that is of importance to the flight control system designer. The maximum allowable $|(q_{cp}/\alpha_g)(j\omega)|$ for Fig. 5 is

$$\left|\frac{q_{cp}}{\alpha_g}(j\omega)\right|_{\max} = \left|\frac{q_{cp_g}}{\alpha_g}(j\omega)\right|_{\max} |T_d(j\omega)| \tag{3}$$

where $(q_{cp_g}/\alpha_g)(j\omega)$ is an open-loop transfer function. Note that the right-hand side of Eq. (3) may not be associated with one particular configuration. That is, $|(q_{cp}/\alpha_g)(j\omega)|_{\max}$ may be associated with different configurations at different frequencies. The $|(q_{cp}/\alpha_g)(j\omega)|_{\max}$ for this study is shown in Fig. 6b. Although this function shows a large amplitude peak, it occurs at a frequency where there is typically little power in the atmospheric turbulence. If necessary, one can reduce $|(q_{cp}/\alpha_g)(j\omega)|$ by reducing $|T_d(j\omega)|$ in the frequency range where the peaking occurs. However, as will be seen, this is not necessary here.

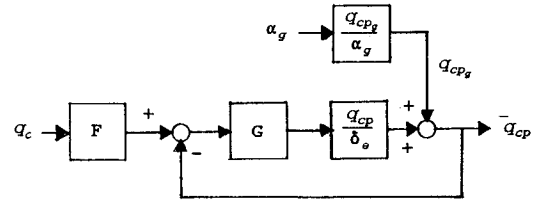


**Fig. 5 System with turbulence disturbance.**

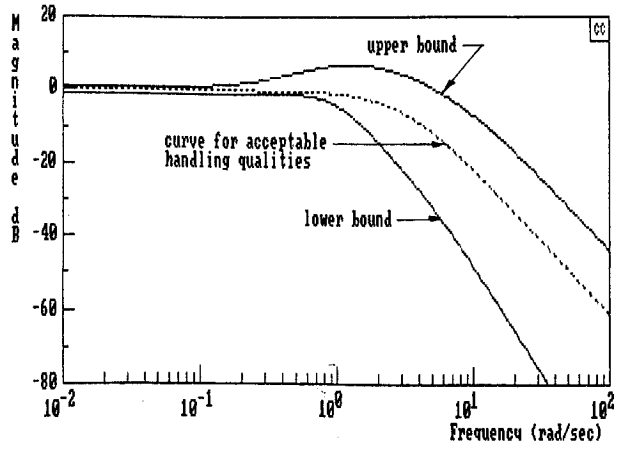


**Fig. 4 Command-following performance boundaries $|(q_{cp}/q_c)(j\omega)|$.**

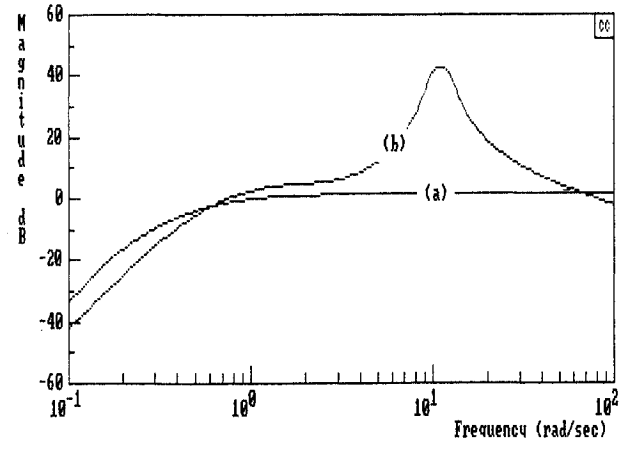


**Fig. 6 Disturbance boundaries: a) $T_d(j\omega)$ and b) $|(q_{cp}/\alpha_g)(j\omega)|_{\max}$.**

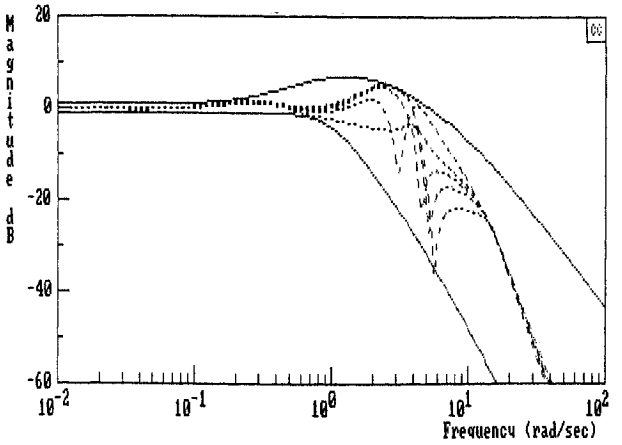


Fig. 7 Command-following performance $|(q_{cp}/q_c)(j\omega)|$.

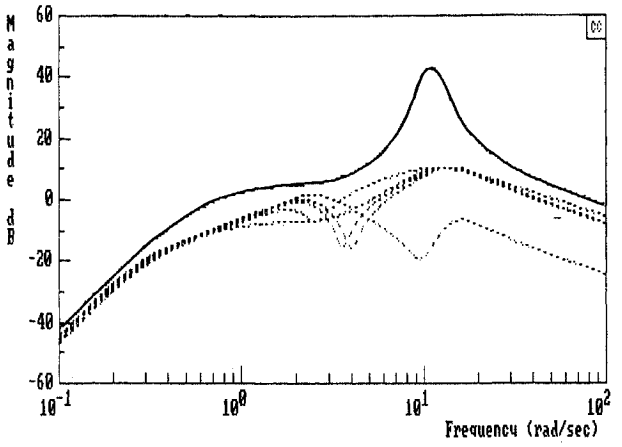


Fig. 8 Disturbance rejection performance $|(q_{cp}/\alpha_g)(j\omega)|$.

### Design Results

Figures 7 and 8 show the command-following and disturbance rejection characteristics of the QFT design for the five vehicle configurations defined in the Appendix. Note that Fig. 8 refers to $|(q_{cp}/\alpha_g)(j\omega)|$. Also note that the reduction in $|T_d(j\omega)|$ alluded to previously is not necessary in this case since the "natural" characteristics of the QFT design eliminate any peaking in response to atmospheric disturbances. The Nichols chart showing the loop transmission for the QFT design is shown in Fig. 9. The loop transmission shown corresponds to the nominal plant (the first listed in the Appendix). Also shown are boundaries $B(j\omega_j)$ at 13 frequencies from 0.1 to 100 rad/s, which the loop transmission must not violate if the command-following and disturbance rejection performance and relative stability requirements are to be obtained despite uncertainty in this frequency range.[8] For clarity, only the frequencies associated with the first four boundaries are identified in the figure. However, all 13 frequencies are identified on the loop transmission. In both QFT designs, stability robustness was ensured by requiring $|L(j\omega)/[1 + L(j\omega)]| \leq 10$ dB and $|1 + L(j\omega)| \geq -4$ dB. Without the former requirement, it is possible for a closed-loop transfer function to remain within the bounds of Fig. 7 while exhibiting an unacceptable magnitude peak. The 10-dB value was somewhat arbitrary here. The latter requirement is synonymous with a gain margin of 8.66 dB and a phase margin of 39 deg. The compensator and prefilter transfer functions are also shown in Table 1. Figure 10 shows the step responses for the design for the five vehicle configurations. With actuator dynamics, the vehicle models are of seventh order. The compensator is seen to be of order 6. As in all QFT designs and as opposed to other design approaches such as those employing $H_\infty$ norms,[12] the order of the compensator is determined by the requirements of the design and not by the order of the plant.

**Table 1 Quantitative feedback theory design results**

| | |
|---|---|
| Prefilter | $\dfrac{175(0.8)(0.6)(3)}{(1)(1.5)^2(7)[0.2, 4]}$ [a] |
| Compensator | $\dfrac{-3.67 \times 10^6(0.22)(0.8)(1.7)(65)}{(0)^2(0.35)[0.7, 160](500)}$ deg-s |

[a] $(b) = (s + b)$; $[\zeta, \omega] = [s^2 + 2\zeta\omega s + \omega^2]$.

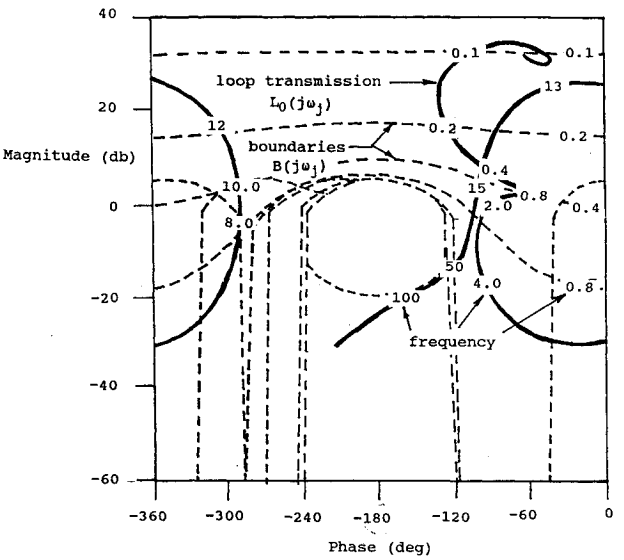


Fig. 9 Nichols chart QFT design.

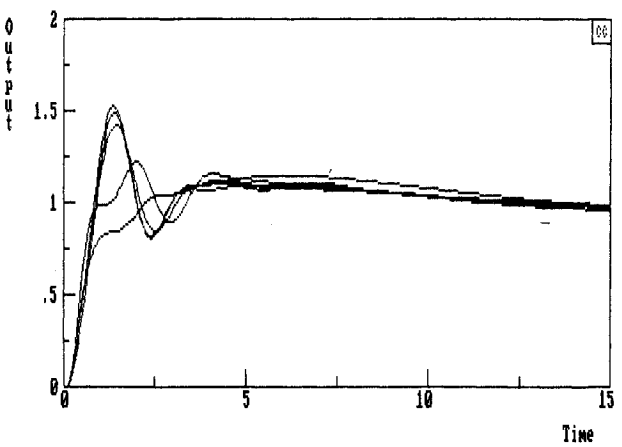


Fig. 10 Unit step responses.

**Table 2 Structural pilot model parameters**

| $K_e$ | $k$ | $K_v$ | $K_1$ | $K_2$ | $T_1$, s | $T_2$, s | $\tau_0$, s | $\zeta$ | $\omega_n$, rad/s |
|---|---|---|---|---|---|---|---|---|---|
| 1.0 | 1 | 0 | 1.0 | 2.0 | 5.0 | NA[a] | 0.15 | 0.707 | 10.0 |

[a] Parameter not applicable.

### Cost of Feedback

Horowitz describes the "cost of feedback" in any design such as this in terms of sensor noise amplification at the plant input.[8] In the critical region beyond open-loop crossover, the sensor noise to control input transfer function $-G(s)S(s)$ is closely approximated by the compensator transfer function itself. An examination of the compensator dynamics beyond crossover in this design indicates a modest cost of feedback. That is, as shown in Fig. 11, the magnitude of the compensator transfer function is nearly constant from 2 to 150 rad/s at a value approximately 8–10 dB below the crossover value and then rapidly rolls off. This is important, since unmodeled elastic modes would not be unduly amplified by this design.

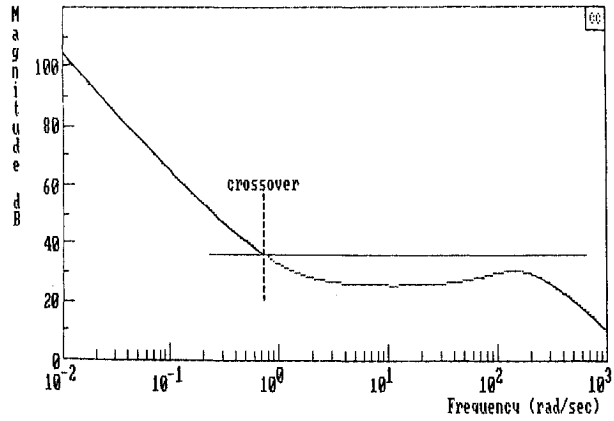


Fig. 11 $|G(j\omega)|$ showing cost of feedback.

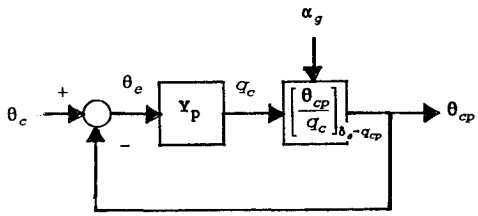


Fig. 12 Pilot–vehicle system for pitch–attitude control where $Y_p$ = structural model of pilot.

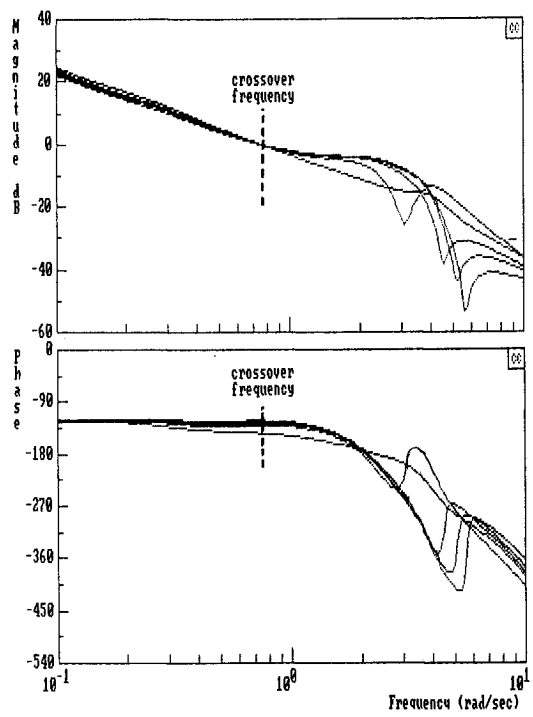


Fig. 13 Loop transmissions for pitch–attitude control $(\theta_{cp}/\theta_e)(j\omega)$.

**Handling Qualities Assessment**

Figure 12 shows the pitch attitude control task with the pilot in the loop. Note that the "effective vehicle" includes the pitch-rate command flight control system whose design was just discussed. Table 2 shows the parameters of the structural model that resulted when the modeling approach discussed in Ref. 10 was applied to the system of Fig. 12. Note that although motion cues were obviously available in the task, for simplicity, they were omitted from the modeling procedure. The pilot gain $K_e$ was unity throughout and the desired crossover frequency was obtained by adjusting the control system gain. As explained in Ref. 10, this procedure removes control sensitivity effects from the handling qualities assessment technique. Figure 13 shows the loop transmissions of the pitch attitude loop for the five vehicle configurations examined herein. Note that the

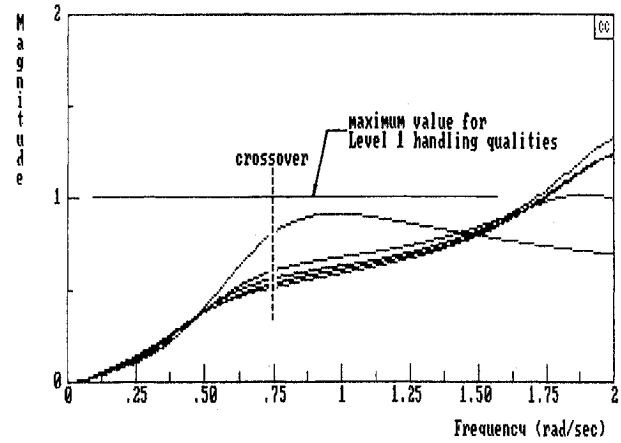


Fig. 14 Handling qualities sensitivity functions.

pilot–vehicle system reflects the well-known "crossover model" of the human pilot.[13]

The pilot model-based assessment of vehicle handling qualities predicted that the elevator-alone design would be level 1 for all configurations. Figure 14 shows the HQSFs for the design. Note that the HQSFs are well below unity in the assumed crossover frequency region (0.75 rad/s).

The question naturally arises at this juncture as to the effect of a task requiring a crossover frequency larger than the assumed 0.75-rad/s value. Note that one cannot simply use the HQSFs of Fig. 14 with a new crossover frequency to answer this question. The structural modeling procedure needs to be repeated. Such an analysis might well predict level 2 handling qualities with one or more of the vehicle configurations. In this case, one would have to increase the bandwidth of the pitch-rate flight control system by suitably modifying Eq. (1) and repeating the QFT design. The tacit and reasonable assumption employed in this study was that any tasks required of the pilot–vehicle system could be satisfactorily accommodated by the nominal pitch-rate system of Eq. (1).

## VI. Conclusions

Based upon the study summarized herein, the following conclusions can be drawn:

1) The QFT design technique allowed a satisfactory longitudinal pitch-rate control system to be designed with uncertain vehicle dynamics that included a lightly damped symmetric body-bending mode. The design employed only a single pitch-rate sensor located near a node of the flexible mode and used only a single aerodynamic control.

2) The use of a structural model of the human pilot allowed handling qualities requirements to be reflected in the performance specifications of the flight control system. In addition, the pilot model could easily assess the handling qualities of the final design.

## Appendix: State-Space Vehicle Models Defining Uncertainty

$$\dot{x}(t) = \boldsymbol{A}x(t) + \boldsymbol{B}u(t)$$

$$y(t) = \boldsymbol{C}x(t) + \boldsymbol{D}u(t)$$

where

$$\{x\} = \{\eta, \dot{\eta}, u, q, \alpha, \theta\}^T$$

$$\{u\} = \{\delta_e, \delta_c\}^T$$

$$\{y\} = q_{cp} = q - \left[\frac{\partial \Phi}{\partial x}\right]_{x=cp} \dot{\eta}$$

Vehicle configuration definitions:

$$A = \begin{bmatrix} 0 & 1 & 0 & 0 & 0 & 0 \\ -153.8 & -0.354 & 0 & -80 & -1076 & 0 \\ 0 & 0 & -0.039 & -2.253 & 19.37 & -32.17 \\ -0.0661 & -0.0038 & 0.0000325 & -0.9445 & -3.4 & 0 \\ -0.0042 & -0.00015 & -0.00032 & 1.0308 & -0.429 & 0 \\ 0 & 0 & 0 & 1 & 0 & 0 \end{bmatrix} \quad B = \begin{bmatrix} 0 & 0 \\ -16.18 & -10.68 \\ 0.261 & 0.0579 \\ -0.0931 & 0.029 \\ -0.00115 & -0.00023 \\ 0 & 0 \end{bmatrix}$$

$$C = [0 \quad 0.03 \quad 0 \quad 1 \quad 0 \quad 0] \qquad D = 0$$

$$A = \begin{bmatrix} 0 & 1 & 0 & 0 & 0 & 0 \\ -100 & -0.5 & 0 & -90 & -1211 & 0 \\ 0 & 0 & -0.022 & -2.535 & 21.79 & -32.174 \\ -0.0744 & -0.004275 & 0.0000366 & -1.06 & -3.825 & 0 \\ -0.004725 & -0.000169 & -0.00036 & 1.16 & -0.4826 & 0 \\ 0 & 0 & 0 & 1 & 0 & 0 \end{bmatrix} \quad B = \begin{bmatrix} 0 & 0 \\ -18.2 & -12.02 \\ 0.293 & 0.0651 \\ -0.105 & 0.0326 \\ -0.0013 & -0.000259 \\ 0 & 0 \end{bmatrix}$$

$$C = [0 \quad 0.03375 \quad 0 \quad 1 \quad 0 \quad 0] \qquad D = 0$$

$$A = \begin{bmatrix} 0 & 1 & 0 & 0 & 0 & 0 \\ -200 & -0.2 & 0 & -70 & -941.5 & 0 \\ 0 & 0 & -0.0439 & -2.535 & 21.79 & -32.174 \\ -0.05783 & -0.00325 & 0.00002844 & -0.82644 & -2.975 & 0 \\ -0.004725 & -0.00016875 & -0.00036 & 1.16 & -0.48263 & 0 \\ 0 & 0 & 0 & 1 & 0 & 0 \end{bmatrix} \quad B = \begin{bmatrix} 0 & 0 \\ -14.158 & -9.345 \\ -0.29329 & 0.0651 \\ -0.081463 & 0.025375 \\ -0.001294 & -0.00025875 \\ 0 & 0 \end{bmatrix}$$

$$C = [0 \quad 0.02625 \quad 0 \quad 1 \quad 0 \quad 0] \qquad D = 0$$

$$A = \begin{bmatrix} 0 & 1 & 0 & 0 & 0 & 0 \\ -173 & -0.39825 & 0 & -90 & -1210.5 & 0 \\ 0 & 0 & -0.075 & -1.9714 & 16.95 & -32.174 \\ -0.0744 & -0.004275 & 0.00003656 & -1.063 & -3.825 & 0 \\ -0.003675 & -0.00013125 & -0.00028 & 0.90195 & -0.3754 & 0 \\ 0 & 0 & 0 & 1 & 0 & 0 \end{bmatrix} \quad B = \begin{bmatrix} 0 & 0 \\ -18.203 & -12.02 \\ 0.22811 & 0.05066 \\ -0.1047 & 0.032625 \\ -0.001006 & -0.00020125 \\ 0 & 0 \end{bmatrix}$$

$$C = \begin{bmatrix} 0 & 0.02625 & 0 & 1 & 0 & 0 \end{bmatrix} \qquad D = 0$$

Actuator dynamics: $75/(s + 75)$.

## References


[1]Ray, L. R., and Stengel, R. F., "Application of Stochastic Robustness to Aircraft Control Systems," *Journal of Guidance, Control, and Dynamics*, Vol. 14, No. 6, 1991, pp. 1251–1259.

[2]Osder, S., and Caldwell, D., "Design and Robustness Issues for Highly Augmented Helicopter Controls," *Journal of Guidance, Control, and Dynamics*, Vol. 15, No. 6, 1991, pp. 1375–1380.

[3]Bilimoria, K., and Schmidt, D., "An Integrated Development of the Equations of Motion for Elastic Hypersonic Flight Vehicles," AIAA Paper 92-4605, Aug. 1992.

[4]Hess, R. A., and Yousefpor, M., "Analyzing the Flared Landing Task with Pitch-Rate Flight Control Systems," *Journal of Guidance, Control, and Dynamics*, Vol. 15, No. 3, 1992, pp. 768–774.

[5]Waszak, M. R., Davidson, J. B., and Schmidt, D. K., "A Simulation Study of the Flight Dynamics of Elastic Aircraft," Vols. 1 and 2, NASA CR-4102, Dec. 1987.

[6]Waszak, W., and Schmidt, D. K., "Flight Dynamics of Aeroelastic Vehicles," *Journal of Aircraft*, Vol. 25, No. 6, 1988, pp. 563–571.

[7]Wykes, J. H., Klepl, M. J., and Brosnan, M. J., "Flight Test and Analyses of the B-1 Structural Mode Control System at Supersonic Flight Conditions," NASA CR 170405, Dec. 1983.

[8]Horowitz, I., "Survey of Quantitative Feedback Theory, (QFT)," *International Journal of Control*, Vol. 53, No. 2, 1991, pp. 255–291.

[9]Yaniv, O., "Multiple-Input Single-Output (MISO) QFT-CAD User Manual," Dept. of Electrical Engineering Systems, Tel-Aviv Univ., Dec. 1991.

[10]Hess, R. A., Malsbury, T., and Atencio, A., "Flight Simulator Fidelity Assessment in a Rotorcraft Lateral Translation Maneuver," *Journal of Guidance, Control, and Dynamics*, Vol. 16, No. 1, 1993, pp. 79–85.

[11]McRuer, D., Ashkenas, I., and Graham, D., *Aircraft Dynamics and Automatic Control*, Princeton Univ. Press, Princeton, NJ.

[12]Maciejowski, J. M., *Multivariable Feedback Design*, Addison–Wesley, Wokingham, England, UK, 1989.

[13]McRuer, D. T., and Krendel, E. S., "Mathematical Models of Human Pilot Behavior," AGARDOgraph No. 188, 1974.